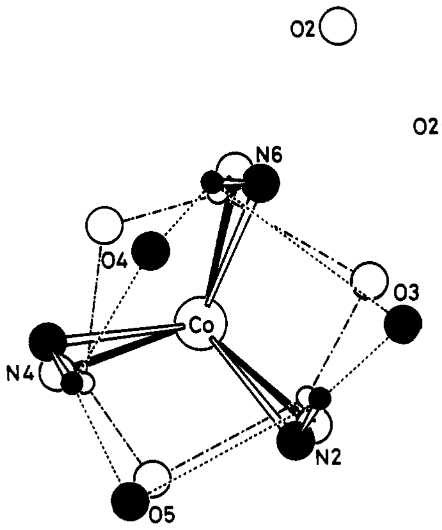

Figure 2. Projection of the four oxygen atoms to the triangular face of the complex cation for Λ-ob_3-[Co(R,R-chxn)$_3$]Cl(d-tart)·3.5H$_2$O (filled circles) and Λ-lel_3-[Co(en)$_3$]Br(d-tart)·5H$_2$O (open circles). The relevant hydrogen bonds are shown by dotted lines.

the three N–H groups and is hydrogen bonded to them simultaneously.[19] A numerical comparison of the hydrogen bonds pertinent to the contact mode is made in Table III.

Now, the above contact mode with the ob_3 complex is examined in detail and is called here the ob_3 contact mode. For comparison, the contact mode found in the crystal of Λ-lel_3-[Co(en)$_3$]Br(d-tart)·5H$_2$O[11] is quoted as the typical lel_3 contact mode, and the hydrogen bonds formed in it are also compared in Table III. To compare the two modes visually, the positions of the four O atoms directed to the complex are projected to the triangular face in Figure 2, such that the three N–H protons of the ob_3 complex may be best superimposed on those of the lel_3 complex.

It is evident in Figure 2 that the two contact modes are surprisingly similar in that the three O atoms are each placed between two of the three N–H groups and are each connected with them through one long and one short hydrogen bond;[14] it is probably due to an intrinsic property of the d-tart ion that its three O atoms are apt to lie among these N–H protons but not just on them.[20] However, the two modes are significantly different with respect to the hydrogen-bond angles (Table III). That is, in the ob_3 contract mode, the three short hydrogen bonds (O3··H–N2, O4··H–N6, and O5··H–N4) are fairly linear and are thus very strong, while the remaining three long ones (O3··H–N6, O4··H–N4, and O5··H–N2) are significantly bent and are thus weak. In the lel_3 contact mode, on the other hand, the three short and three long hydrogen bonds are all moderately bent, though the longer ones tend to be more bent[21] as in the ob_3 contact mode. These differences are to be expected, because when the conformation is changed from lel_3 to ob_3, with the three O atoms left almost intact, each N–H proton comes to be in a position to form a shorter and more linear hydrogen bond to one O atom and a longer and more bent hydrogen bond to the other O atom. As a result, of the six moderately bent hydrogen bonds formed in the lel_3 mode, the three short ones are strengthened but the three long ones are weakened upon the conformational change to ob_3. In this way, since the ob_3 contact mode found here is quite reasonable, this mode is likely to be adopted in solution as well.

Some pieces of experimental evidence are available which indicate that the d-tart ion shows a weaker affinity for the ob_3 complex in solution,[6,13] like the usual oxo anions do. Then, if the d-tart ion adopts in solution the contact modes similar to those shown in Figure 2, the overall hydrogen-bonding interaction in the ob_3 mode must be surpassed by that in the lel_3 mode. However, since the three short and three long hydrogen bonds formed in the lel_3 mode are further strengthened and weakened, respectively, upon the conformational change to ob_3, the overall interaction is not so drastically diminished in the ob_3 mode. In contrast, the usual oxo anions suffer a serious damage to their hydrogen-bonding interaction with the complex upon the conformational change; the three originally linear and strong hydrogen bonds are all forced to be bent and are weakened appreciably.[22] Therefore, it is expected that the usual oxo anions serve as a more effective selector than d-tart ion in the chromatographic separation of these conformational isomers.[23] Our preliminary study has estimated the conventional separation factor[13] to be 2.38 for Na$_2$SO$_4$ (0.1 M) and 1.88 for Na$_2$$d$-tart (0.1 M) in the chromatographic separation of Λ-lel_3- and Λ-ob_3-[Co(chxn)$_3$]$^{3+}$ on an SP-Sephadex ion-exchange column. These experimental results are consistent with our assertion that the usual oxo anions are more readily subjected to the effect of the chelate conformation, when they form ion pairs with these metal–amine complex cations through the hydrogen-bonding interaction.[8,10,23] In contrast, the d-tart ion is rather insensitive to the conformational change; it manages to form intimate hydrogen bonds to both lel_3 and ob_3 complexes.

Supplementary Material Available: Full listings of the crystallographic data (Table ST1), positional and isotropic thermal parameters for hydrogen atoms (Table ST2), bond distances and angles (Table ST3), and anisotropic thermal parameters for non-hydrogen atoms (Table ST4) (7 pages); a listing of observed and calculated structure factor amplitudes (Table ST5) (17 pages). Ordering information is given on any current masthead page.

---

(19) The second hydrogen bond (O3··H–N6) in the ob_3 contact mode given in Table III might be too long to be regarded as an actual bond.

(20) Yoneda, H. *J. Chromatogr.* **1984**, *313*, 59.

(21) Taylor, R.; Kennard, O. *Acc. Chem. Res.* **1984**, *17*, 320.

(22) For example: Vedani, A.; Dunitz, J. D. *J. Am. Chem. Soc.* **1985**, *107*, 7653.

(23) Searle, G. H. *Aust. J. Chem.* **1977**, *30*, 2625.

Contribution from the Department of Chemistry,
Oregon State University, Gilbert Hall 153,
Corvallis, Oregon 97331-4003

The Cubane Structure of $Mo_4O_4(\mu_3\text{-}O)_4(OSi(CH_3)_3)_4(HN(CH_3)_2)_4$[†]

Gyu Shik Kim, Douglas A. Keszler,* and Carroll W. DeKock*

Received April 3, 1990

Introduction

Compounds of transition-metal clusters, that is compounds containing metal–metal bonds, have been actively studied over the last two decades.[1] Among these molecules, the cubane structure containing the core $M_4(\mu_3\text{-}X)_4$ has been an important and recurrent structural motif in a number of molecular systems, having now been observed with the metals M = V, Cr, Mo, W, Re, Fe, Os, Co, and Pt bound by a variety of ligands. Also, the oxo Mo cubane $Mo_4(\mu_3\text{-}O)_4$ has recently been observed in condensed oxide phases, forming in layered structures[2] and three-dimensional microporous solids.[3] In all these systems, the cubane may be highly distorted, with the nature of the distortions arising from the number of electrons available for bonding and the characteristics of the ligands.[4,5]

Our recent interests have involved the preparation of new oxo Mo compounds by the cocondensation of MoO$_3$ and various silicon reagents; these syntheses have afforded a variety of new dioxo–alkoxo (siloxo)–Mo compounds.[6] Here we wish to describe the structure and synthesis of the new compound $Mo_4O_4(\mu_3\text{-}O)_4(OSi(CH_3)_3)_4(HN(CH_3)_2)_4$, which was crystallized as a minor

---

[†] This work was presented at the 43rd Northwest Regional Meeting of the American Chemical Society, Spokane, Washington, June 29–July 1, 1988; INORG 128.

Table I. Crystal Data and Experimental Conditions for $Mo_4O_4(\mu_3\text{-}O)_4(OSi(CH_3)_4(HN(CH_3)_2)_4$

fw	1037.76	Z	8
space group	$P2_1/c$ (No. 14)	ρ_{calcd}, g cm^{-1}	1.51
a, Å	20.248 (4)	T, K	295
b, Å	20.151 (6)	μ(Mo Kα), cm^{-1}	11.99
c, Å	24.576 (7)	R(on F for F_o^2 > $3\sigma(F_o^2)$)	0.061
β, deg	114.14 (2)		
V, Å^3	9150 (4)	$R_w(F)$	0.068

product in the cocondensation of the reagents MoO_3 and $(CH_3)_3SiN(CH_3)_2$. The compound is a rare example of an oxo tetranuclear Mo(V) cluster that exists as an oxo Mo cubane;[7] to our knowledge it is the first example of a molecular cubane with Mo(V) supported only by monodentate ligands to be structurally characterized. The distortions within the core are consistent with the electron configuration of the Mo atom and the electron-donating abilities of the ligands.

Experimental Section

Synthesis. The title compound was prepared by the cocondensation of MoO_3 (16.7 mmol) and $(CH_3)_3SiN(CH_3)_2$ (215 mmol) at 77 K following procedures reported elsewhere.[6] Red crystals were isolated from a toluene extract of the cocondensate. The crystal used for the collection of X-ray data (vide infra) was recrystallized from toluene. Anal. Calcd for $C_{20}H_{64}N_4O_{12}Mo_4$: C, 22.90; H, 6.15; N, 5.34; Mo, 36.59. Found: C, 22.93; H, 6.13; N, 5.03; Mo, 36.49. ^1H NMR (400 MHz, in toluene-d_8, referenced to the solvent at 2.09 ppm): δ 0.38 (s, 9 H, $OSi(CH_3)_3$), 2.61 (d, 3 H, NMe_A, J_{H-H} = 5.7 Hz), 2.72 (d, 3 H, NMe_B, J_{H-H} = 5.7 Hz), 7.24 (sept, 1 H, NH, J_{H-H} = 5.7 Hz). Electronic spectrum (in toluene solution, 1-cm cell): λ_{max} 352 nm (ϵ = 3420), 472 nm (ϵ = 790). Mass spectral data, m/z [% int, assgn]: 308 [100, $MoO_2(OSi(CH_3)_3)_2^{2-}$], 434 [3, $Mo_2O_4(OSi(CH_3)_3)_2^-$], 612 [8, $Mo_2O_4(OSi(CH_3)_3)_4^-$], 779 [2, $Mo_4O_8(OSi(CH_3)_3)_3^-$], 868 [50, $Mo_4O_8(OSi(CH_3)_3)_4^-$].

X-ray Work. A red, crystalline plate of dimensions 0.3 × 0.3 × 0.15 mm was used for collection of data. Unit cell parameters were derived from a least-squares analysis of the angle settings of 20 reflections in the range $11° \leq 2\theta \leq 14°$ that were automatically centered on a Rigaku AFC6R diffractometer. Intensity data were collected with the ω–2θ scan technique with a scan speed of 16°/min in ω and a scan width $\Delta\omega = (0.92 + \tan\omega)°$. The intensities of three standard reflections monitored throughout data collection exhibited fluctuations below 2%. From the 13 486 reflections measured to $(\sin\theta_{max})/\lambda$ = 0.595 Å^{-1} in the range of indices $-24 \leq h \leq 24$, $0 \leq k \leq 24$, $0 \leq l \leq 29$, 3312 unique data with $F_o^2 \geq 3\sigma(F_o^2)$ were obtained.

Table II. Positional Parameters and B_{eq} for $Mo_4O_4(\mu_3\text{-}O)_4(OSi(CH_3)_3)_4(HN(CH_3)_2)_4$

	x	y	z	B_{eq}, Å^2
Mo(1)	0.1758 (1)	0.2127 (1)	0.2348 (1)	4.0 (1)
Mo(2)	0.1717 (1)	0.3404 (1)	0.2165 (1)	3.7 (1)
Mo(3)	0.3426 (1)	0.2850 (1)	0.2989 (1)	3.8 (1)
Mo(4)	0.3027 (1)	0.2634 (1)	0.1853 (1)	3.8 (1)
Mo(11)	0.7567 (2)	0.2028 (1)	0.2960 (1)	4.0 (1)
Mo(12)	0.7325 (2)	0.2118 (1)	0.1840 (1)	4.1 (1)
Mo(13)	0.6896 (1)	0.3552 (1)	0.2374 (1)	4.0 (1)
Mo(14)	0.8279 (1)	0.3443 (1)	0.2656 (1)	4.1 (1)
Si(1)	0.1691 (6)	0.1246 (5)	0.3453 (5)	6.5 (6)
Si(2)	0.0886 (5)	0.4287 (5)	0.0961 (5)	5.5 (5)
Si(3)	0.4131 (6)	0.4178 (5)	0.3829 (5)	6.0 (5)
Si(4)	0.3131 (6)	0.1306 (5)	0.1091 (5)	6.8 (6)
Si(11)	0.6480 (6)	0.1618 (5)	0.3598 (5)	6.2 (5)
Si(12)	0.8318 (6)	0.1709 (5)	0.1114 (5)	6.1 (5)
Si(13)	0.5539 (6)	0.4109 (5)	0.1158 (5)	6.7 (6)
Si(14)	0.9672 (6)	0.3691 (5)	0.3954 (5)	6.8 (6)
O(1)	0.089 (1)	0.203 (1)	0.2195 (8)	5.0 (5)
O(2)	0.087 (1)	0.3522 (9)	0.2059 (9)	5.2 (5)
O(3)	0.431 (1)	0.2784 (9)	0.3193 (8)	4.7 (5)
O(4)	0.386 (1)	0.267 (1)	0.1876 (8)	5.1 (5)
O(5)	0.2213 (9)	0.2861 (8)	0.2891 (7)	3.5 (4)
O(6)	0.178 (1)	0.2661 (8)	0.1686 (7)	3.7 (4)
O(7)	0.2929 (9)	0.3412 (8)	0.2301 (7)	3.3 (4)
O(8)	0.300 (1)	0.2063 (8)	0.2500 (8)	3.9 (4)
O(11)	0.212 (1)	0.1560 (9)	0.3068 (8)	4.2 (4)
O(12)	0.163 (1)	0.3988 (8)	0.1491 (8)	3.5 (4)
O(13)	0.349 (1)	0.3637 (9)	0.3502 (8)	4.5 (5)
O(14)	0.268 (1)	0.1861 (8)	0.1286 (8)	4.4 (5)
O(21)	0.759 (1)	0.120 (1)	0.299 (1)	6.2 (6)
O(22)	0.715 (1)	0.133 (1)	0.168 (1)	6.1 (5)
O(23)	0.690 (1)	0.4369 (9)	0.2466 (8)	4.5 (5)
O(24)	0.844 (1)	0.4249 (9)	0.2659 (8)	4.6 (5)
O(25)	0.741 (1)	0.3282 (8)	0.1891 (8)	3.9 (4)
O(26)	0.772 (1)	0.3188 (8)	0.3102 (8)	4.1 (5)
O(27)	0.818 (1)	0.2242 (9)	0.2533 (8)	4.2 (4)
O(28)	0.676 (1)	0.2385 (8)	0.2288 (8)	4.3 (5)
O(31)	0.700 (1)	0.213 (1)	0.3444 (8)	5.3 (5)
O(32)	0.791 (1)	0.2262 (9)	0.1368 (8)	4.6 (5)
O(33)	0.598 (1)	0.354 (1)	0.1607 (9)	5.4 (5)
O(34)	0.915 (1)	0.323 (1)	0.3397 (9)	5.4 (5)
N(1)	0.173 (1)	0.131 (1)	0.177 (1)	4.4 (6)
N(2)	0.213 (1)	0.424 (1)	0.280 (1)	5.2 (6)
N(3)	0.346 (1)	0.218 (1)	0.370 (1)	5.4 (6)
N(4)	0.258 (1)	0.332 (1)	0.110 (1)	5.3 (6)
N(11)	0.859 (1)	0.212 (1)	0.374 (1)	5..0 (6)
N(12)	0.632 (2)	0.241 (1)	0.109 (1)	7.3 (8)
N(13)	0.629 (1)	0.336 (1)	0.291 (1)	5.9 (7)
N(14)	0.888 (1)	0.321 (1)	0.211 (1)	4.3 (6)

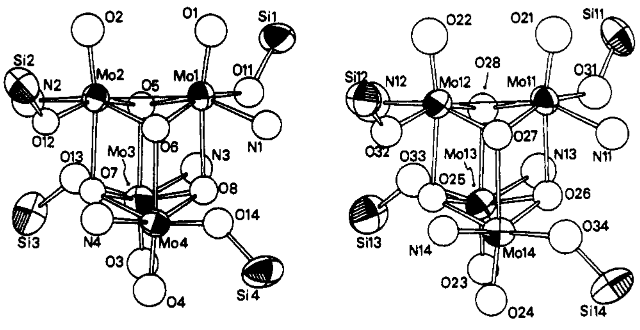

Figure 1. Labeled drawing of the two molecules in the structure of $Mo_4O_4(\mu_3\text{-}O)_4(OSi(CH_3)_3)_4(HN(CH_3)_2)_4$.

All calculations were performed on a MicroVAX II computer with programs from the TEXSAN crystallographic software package.[8] The positions of the Mo atoms were determined from the direct-methods program MITHRIL.[9] All remaining non-hydrogen atoms were located in a subsequent application of the difference direct-methods program DIRDIF;[10] H atoms were placed in calculated positions. An absorption correction was made by use of the program DIFABS.[11] Final least-squares refinement on F_o with anisotropic thermal parameters on the atoms Mo and Si and isotropic parameters on the atoms C, N, and O affords the residuals R = 0.061 and R_w = 0.068. The final difference electron density map contains a maximum feature of 0.71 e/Å^3. Crystal data and experimental conditions are summarized in Table I. Final atomic positions are listed in Table II.

The monoclinic cell may be transformed by application of the matrix [−1 0 0, 1 0 2, 0 1 0] to a cell that is approximately C-centered orthorhombic with the cell parameters a = 20.248 Å, b = 44.852 Å, c = 20.15 Å, $\alpha = \beta$ = 90°, and γ = 90.18°. Analysis of the magnitudes of the structure factors following transformation to the orthorhombic setting reveals several violations of Laue symmetry *mmm*. Examination of atomic coordinates and drawings of the structure in the orthorhombic cell

---

(1) Garner, C. D. *Transition Metal Clusters*; Johnson, B. F. G., Ed.; Wiley: New York, 1980; pp 265–344.

(2) Corcoran, E. W., Jr. *Inorg. Chem.* **1990**, *29*, 157.

(3) Haushalter, R. C.; Strohmaier, K. G.; Lai, F. W. *Science* **1989**, *246*, 1289.

(4) Cotton, F. A.; Wilkinson, G. *Advanced Inorganic Chemistry*; Wiley Interscience: New York, 1988; Chapter 23.

(5) Williams, P. D.; Curtis, M. D. *Inorg. Chem.* **1986**, *25*, 4562.

(6) Kim, G. S.; Huffman, D.; DeKock, C. W. *Inorg. Chem.* **1989**, *28*, 1279.

(7) For an example of an oxo Mo cubane with a bidentate ligand, see: Mattes, R.; Mühlsiepen, K. *Z. Naturforsch., B: Anorg. Chem., Org. Chem.* **1980**, *35*, 265.

(8) Molecular Structure Corp. *TEXSAN, Texray Structure Analysis Package*; MSC: 3200 A Research Forest Drive, The Woodlands, TX 77381.

(9) Gilmore, G. J. *MITHRIL: A Computer Program for the Automatic Solution of Crystal Structures from X-ray Data*; University of Glasgow: Glasgow, Scotland, 1983.

(10) Beurskens, P. T. *DIRDIF: Direct Methods for Difference Structures*; Technical Report 1984/1; Crystallography Laboratory: Toernooiveld, 6525 Ed Nijmegen, The Netherlands.

(11) Walker, N.; Stuart, D. *Acta Crystallogr., Sect. A* **1968**, *24*, 214.

Table III. Bond Distances (Å) for $Mo_4O_4(\mu_3\text{-}O)_4(OSi(CH_3)_3)_4(HN(CH_3)_2)_4$

molecule I		molecule II	
Mo(1)–Mo(2)	2.607 (4)	Mo(11)–Mo(12)	2.599 (4)
Mo(3)–Mo(4)	2.606 (4)	Mo(13)–Mo(14)	2.606 (4)
Mo(1)–O(1)	1.66 (2)	Mo(11)–O(21)	1.67 (2)
Mo(2)–O(2)	1.68 (2)	Mo(12)–O(22)	1.63 (2)
Mo(3)–O(3)	1.66 (2)	Mo(13)–O(23)	1.66 (2)
Mo(4)–O(4)	1.66 (2)	Mo(14)–O(24)	1.66 (2)
Mo(1)–O(5)	1.95 (2)	Mo(11)–O(27)	1.97 (2)
Mo(1)–O(6)	1.97 (2)	Mo(11)–O(28)	1.93 (2)
Mo(2)–O(5)	1.96 (2)	Mo(12)–O(28)	1.96 (2)
Mo(2)–O(6)	1.94 (2)	Mo(12)–O(27)	1.89 (2)
Mo(3)–O(7)	1.94 (2)	Mo(13)–O(25)	1.95 (2)
Mo(3)–O(8)	1.96 (2)	Mo(13)–O(26)	2.02 (2)
Mo(4)–O(7)	1.97 (2)	Mo(1)–O(26)	1.94 (2)
Mo(4)–O(8)	1.98 (2)	Mo(14)–O(25)	2.00 (2)
av	1.96	av	1.96
Mo(1)–O(8)	2.38 (2)	Mo(11)–O(26)	2.36 (2)
Mo(2)–O(7)	2.34 (2)	Mo(12)–O(25)	2.35 (2)
Mo(3)–O(5)	2.37 (2)	Mo(13)–O(28)	2.37 (2)
Mo(4)–O(6)	2.38 (2)	Mo(14)–O(27)	2.44 (2)
av	2.37	av	2.38
Mo(1)–N(1)	2.16 (2)	Mo(11)–N(11)	2.19 (2)
Mo(2)–N(2)	2.21 (2)	Mo(12)–N(12)	2.19 (2)
Mo(3)–N(3)	2.18 (2)	Mo(13)–N(13)	2.18 (2)
Mo(4)–N(4)	2.20 (2)	Mo(14)–N(14)	2.20 (2)
av	2.19	av	2.19
	Ligands (Average Only)		
Si–O	1.64	Si–O	1.63
Si–C	1.84	Si–C	1.84
C–N	1.46	C–N	1.48

does not reveal symmetry operations consistent with the supergroup *Cmca* of any other *C*-centered orthorhombic group. Hence, we conclude the monoclinic description $P2_1/c$ to be correct.

Results and Discussion

The compound crystallizes with two molecules per asymmetric unit; an ORTEP drawing of the molecules is shown in Figure 1. Bond distances are listed in Table III. As shown by inspection of Table III, the two independent molecules do not differ by more than three standard deviations in any distance. Each molecule has approximate S_4 symmetry, and the $Mo_4(\mu_3\text{-}O)_4$ cores exhibit approximate D_{2d} symmetry even though the symmetry is not crystallographically imposed. Each Mo atom occupies a distorted octahedral environment similar to that in solid MoO_3.[12] Triply bridging O atoms occupy alternating corners of the cubane core; the average Mo-μ_3-O bond distances 1.94 Å (trans to N), 1.98 Å (trans to OSi), and 2.38 Å (trans to terminal O) are consistent with the trans influences of the ligands. Two Mo–Mo distances at 2.605 Å and four distances at 3.42 Å span the six face diagonals of the cube. The Mo–Mo distance, 2.605 Å, corresponds to a Mo–Mo single bond,[13] while the distance 3.42 Å represents a nonbonding Mo···Mo interaction.

The Mo–O–Si bond angles near 131 (1)° are similar to those, 134.1 (3) and 136.4 (3)°, reported for the two siloxo groups that are trans to the N atoms of the amines in the dimer $Mo_2(OSi(CH_3)_6(HN(CH_3)_2)_2$.[14] Values for the remaining siloxo groups of the dimer that are trans to one another range from 156 to 176°; these values compare wtih the Si–O–Si angle of 148° reported for hexamethyldisiloxane.[15] Because the trimethylsilyl groups do not appear to be sterically congested in these compounds, the acute angles likely arise from an electronic effect.

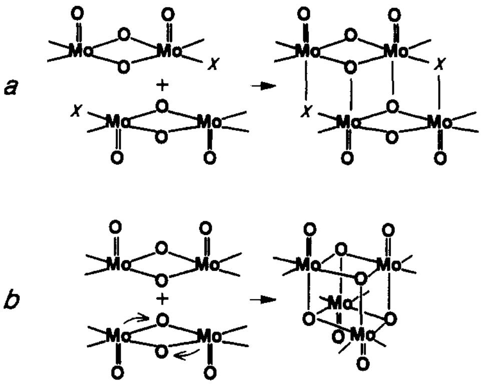

Figure 2. (a) Fusion of two oxo-bridged dimers to form a bioctahedron. (b) Fusion of two oxo-bridged dimers to form a cubane.

Each set of siloxo and dimethylamine groups is structurally equivalent as revealed by consideration of the limits of error in the interatomic distances and angles as well as the ^1H NMR spectrum. The Mo–N, Si–C, and N–C distances are quite normal, and the Mo–N–C, C–N–C, O–Si–C, and C–Si–C angles indicate sp^3-bonded Si and N.

Related Structures. Two oxo Mo structures, the bioctahedron and cubane, which result from condensation of dioxo-bridged metal fragments are diagrammed in Figure 2. The fused bioctahedral structure of Figure 2a has been reported for a number of transition-metal (oxo) alkoxo complexes. For example, the compound $Ti_4(OR)_{16}$ with no metal–metal bonds as well as the compounds $W_4(OR)_{16}$ (R = Me, Et),[16] $Mo_4O_8(O\text{-}i\text{-}Pr)_4(py)_4$,[17] and relatives of the core $[Mo_4O_8(OR)_4Cl_4]^{2-}$ [18-21] with metal–metal bonds exhibit this structure. In the fused bioctahedral complex $Mo_4O_8(OEt)_2(tme)$[22] (tme = $CH_3C(CH_2O)_3)^{3-}$) containing Mo(VI), two tridentate ligands bind the four Mo atoms to afford the Mo–Mo distances, 3.44, 3.49, and 3.70 Å, all corresponding to nonbonded interactions; one O atom of each tme ligand occupies a triply bridging site.

Condensation to form the cubane structure is depicted in Figure 2b. Examples of molecular oxo Mo cubes are less common, being represented by the title compound and the molecule $Mo_4O_8((CH_3)_2POS)_4$.[7] In the cubane four triply bridging ligands link the Mo atoms in the core whereas in the bioctahedral arrangement only two of the four oxo groups are triply bridging, and two additional doubly bridging X groups are present to link the Mo atoms. What factors favor the formation of the cubane or the bioctahedron? One factor is the ability of the X group to bridge the Mo atoms in the bioctahedral arrangement. Oxo and alkoxo ligands readily bridge these metal atoms whereas substituted amines and siloxo groups exhibit a lower tendency to do so. The nature of complexes with N ligands is demonstrated by the molecule $Mo_4O_4(\mu\text{-}O)_4(\mu\text{-}O(CH_3)_2(HB(pz)_3)_2(CH_3OH)_2$[23] containing Mo(V) and a tridentate polypyrazoylborate ligand. This complex does not crystallize as a bioctahedron or cubane, adopting instead an oligomeric structure that is capped at each end by the tridentate N ligand. As in the case of the title compound, the N ligand does not bridge the metal atoms; only a single pair of electrons is available for donation. The lack of a bridging capacity for the ligand N atoms prevents the more compact association in a bioctahedral arrangement. Siloxo groups have been observed

---

(12) Wells, A. F. *Structural Inorganic Chemistry*; Clarendon: Oxford, U.K., 1984.

(13) (a) Metallic Mo–Mo bond is 2.592 Å: Pauling, L. *The Nature of the Chemical Bond*, 3rd ed.; Cornell University Press: Ithaca, NY, 1960; p 440. (b) Cotton, F. A. In *Reactivity of Metal-Metal Bonds*; Chisholm, M. H., Ed.; ACS Symposium Series 155; American Chemical Society: Washington, DC, 1981; pp 1–16. (c) Chisholm, M. H. *Polyhedron* **1983**, *2*, 681.

(14) Chisholm, M. H.; Extine, M. W.; Reichert, W. W.; Thornton, P. *J. Am. Chem. Soc.* **1978**, *100*, 153.

(15) Csakvari, B.; Wagner, Z. S.; Gömöry, P. *J. Organomet. Chem.* **1976**, *107*, 287.

(16) Chisholm, M. H.; Huffman, J. C.; Leonelli, J. *J. Chem. Soc., Chem. Commun.* **1981**, 270.

(17) Chisholm, M. H.; Huffman, J. C.; Kirkpatrick, C. C.; Leonelli, J.; Folting, K. *J. Am. Chem. Soc.* **1981**, *103*, 6093.

(18) Liu, S.; Zubieta, J. *Polyhedron* **1989**, *8*, 537.

(19) Hsieh, T.-C.; Zubieta, J. *J. Chem. Soc., Chem. Commun.* **1985**, 1749.

(20) Hsieh, T.-C.; Shaikh, S. N.; Zubieta, J. *Inorg. Chem.* **1987**, *26*, 4079.

(21) Kang, H.; Liu, S.; Shahid, N. S.; Nicholson, T.; Zubieta, J. *Inorg. Chem.* **1989**, *28*, 920.

(22) Wilson, A. J.; Robinson, W. T.; Wilkins, C. J. *Acta Crystallogr., Sect. C* **1983**, *39*, 54.

(23) Koch, S. A.; Lincoln, S. *Inorg. Chem.* **1982**, *21*, 2904.

to bridge in only one Mo complex, and the interactions are weak.[6] Ligands such as oxo and alkoxo exhibit a greater ability to donate electron density and bridge compared with siloxo, since a greater proportion of the O electron density in the siloxo group is locked into strong Si–O bonding interactions within the ligand, making it unavailable for bonding. It appears to us that the title compound crystallizes as a cubane, in part, because the strong bridging ability of the oxo groups in conjunction with the comparatively weaker bridging ability of the siloxo group prevents the formation of the bioctahedral structure.

Why should the cubane or bioctahedron form rather than some other more open structure? Representatives of open structures include the forementioned pyrazoylborate and the complex $Mo_4O_4(\mu_3\text{-}O)Cl_2(CH_3COO)_6$.[24] The structure of the latter molecule may be constructed from one of the simple dimer units depicted at the left in Figure 2 and two additional Mo-centered octahedra, each attached to one of the shared O vertices of the dimer. These vertices are the only ligand atoms shared among the Mo atoms. In the cubane and fused bioctahedral structures, the ratio of donor atoms:metal atoms is fixed at 4:1. Comparing the open structures with the bioctahedron and cubane, we find fewer ligand atoms occupying bridging positions in the open structures. If fewer atoms are bridging, a greater number of ligand atoms will be required to fill the resulting terminal sites and complete the octahedral coordination about each Mo atom. Hence, a larger ratio of donor atoms:metal atoms, 9:2, is observed in the open structures. If the bridging abilities of the ligand atoms are limited, a larger number of ligand atoms will be required, and the bioctahedron and cubane will not form. The ratio of donor atoms:metal atoms as dictated by the bridging and electron-donating abilities of the ligands affords the cubane structure of the title compound.

Acknowledgment. D.A.K. thanks the Alfred P. Sloan Research Foundation for a fellowship (1989–1991).

Supplementary Material Available: Table S-1, listing complete crystal and experimental data, Table S-2, giving positional parameters, Table S-3, listing *U* values, Table S-4, giving intramolecular interatomic distances, and Table S-5, listing intramolecular interatomic angles (16 pages); Table S-6, listing calculated and observed structure factors (23 pages). Ordering information is given on any current masthead page.

---

(24) Kamenar, B.; Korpar-Colig, B.; Penavic, M. *J. Chem. Soc., Dalton Trans.* **1981**, 311.

Contribution from Ultrasystems Defense, Inc.,
16775 Von Karman Avenue, Irvine, California 92714

Novel Trimethylsilyl-Substituted Aminoboranes

K. J. L. Paciorek,* S. R. Masuda, L. A. Hoferkamp,
J. H. Nakahara, and R. H. Kratzer

Received May 1, 1990

The major emphasis in the approaches to BN precursors has been centered on cyclics.[1] However, as demonstrated by Beck et al., reaction of simple adducts such as $Me_2S{\cdot}BHBr_2$ with ammonia provide alternate routes to BN.[2] Trimethylsilyl-substituted aminoboranes are also of potential interest in this application in view of their processibility, versatility, and the ease of (trimethylsilyl)amino group elimination. A number of (trimethylsilyl)amino-substituted boranes have been described.[3-10] We have prepared a bis((silylamino)boryl)amine, $[(Me_3Si)_2NBNHSiMe_3]_2NH$;[11] however, the feasibility of making longer chain B–N materials of this nature needed to be established. Shaw et al.[12] approached this problem by bridging N–B(Ph)–N with $(CH_2)_n$ units. The presence of carbon on nitrogen and boron in this system provides for carbon retention on any subsequent pyrolysis. In BN precursors a very important consideration is the avoidance of carbon substituents on boron. Earlier, Jenne and Niedenzu[13] and Nöth and co-workers[14,15] described a series of noncyclic boron–nitrogen compounds containing up to four boron atoms. However, in each of the compounds, at least some of the boron atoms were either alkyl- or aryl-substituted. Our goal was to prepare B–N chains free of B–C and N–C linkages. We wish now to report novel linear borylamines containing up to four boron atoms as well as intermediates containing free NH_2 substituents. The latter offer particularly suitable monomers for linear B–N polymer synthesis and borazine-ring-linking applications.

Experimental Section

General Procedures. Operations were carried out either in an inert-atmosphere enclosure (Vacuum/Atmospheres Model HE-93B), under nitrogen bypass, or by using standard vacuum line procedures.[16] Infrared spectra were recorded: solids as double mulls (Kel-F oil No. 10 and Nujol); liquids as capillary films on a Perkin-Elmer Model 1330 infrared spectrophotometer. The mass spectra (EI) were obtained from a Du Pont Model 21-491B spectrometer. The spectrometer was attached to a Varian Aerograph Model 2700 gas chromatograph equipped with a flame ionization detector and a Du Pont 21-094 data acquisition and processing system. Gas chromatography was performed by employing a 3 ft × $^1/_8$ in. stainless steel column packed with 3% Dexsil 300 resin on 100/200 mesh Chromosorb W-AW. NMR spectra were recorded on a Varian VXR-200 spectrometer; for ^{11}B a 64.2-MHz operating frequency was employed. Me_4Si and $BF_3{\cdot}Et_2O$ were used as external standards for ^1H and ^{11}B NMR, respectively. Boron and nitrogen were determined by wet analysis; boron by base titration, nitrogen as NH_3 by using ion chromatography.

Materials. Ammonia (Matheson Gas Products) was purified by trap-to-trap distillation and dried over potassium, and BCl_3 by vacuum line fractional condensations; $(Me_3Si)_2NH$ (Aldrich Chemical Co.) was used as received; triethylamine (Aldrich Chemical Co.) was distilled from $LiAlH_4$. $(Me_3Si)_2NB(NH_2)NHSiMe_3$,[6] $(Me_3Si)_2NBCl_2$,[5] and $BCl_3{\cdot}NEt_3$[17] were prepared by literature procedures. All solvents were rigorously dried and degassed.

$(Me_3Si)_2NB[HNB(NHSiMe_3)N(SiMe_3)_2]_2$ (1). To a stirred solution of $(Me_3Si)_2NB(NH_2)NHSiMe_3$ (14.99 g, 54.4 mmol) in triethylamine (38 mL) was added dropwise, at room temperature, $(Me_3Si)_2NBCl_2$ (6.61 g, 27.3 mmol) over a period of 30 min; a white precipitate started to form immediately. Stirring was continued for 16 h at room temperature, followed by 6.5 h at 100 °C. After cooling, triethylamine hydrochloride, 4.15 g (55.4% yield), was filtered off. The excess triethylamine, unreacted starting materials, and byproducts were removed in vacuo by heating to 213 °C. Some of the product (13% of theoretical yield based on $(Me_3Si)_2NBCl_2$ employed) was present in the distillate as determined by GC. The product accounted for 87% of the 3.82 g of distillation residue, bringing the total yield of the material to 21.5%. Crystallization from Freon-113 gave 1.57 g of $(Me_3Si)_2NB[HNB(NHSiMe_3)N(SiMe_3)_2]_2$, mp 120–120.5 °C. Anal. Calcd for $C_{24}H_{76}N_7B_3Si_8$: N, 13.62; B, 4.50. Found: N, 13.93; B, 4.54. IR (cm^{-1}, NaCl plates): 3395 (w), 3360 (w), 3300 (m), 2950 (s), 2895 (m), 1410 (s, br), 1346 (s), 1260 (s), 1247 (s), 1143 (m), 1108 (s), 996 (s), 965 (sh),

---

(1) Paine, R. T.; Narula, C. K. *Chem. Rev.* **1990**, *90*, 73 and references therein.

(2) Beck, J. S.; Albani, C. R.; McGhie, A. R.; Rothman, J. B.; Sneddon, L. G. *Chem. Mater.* **1989**, *1*, 433.

(3) Steinberg, H.; Brotherton, R. J. *Organoboron Chemistry*; Wiley and Sons: New York, 1966; Vol. II.

(4) Geymayer, P.; Rochow, E. G. *Monatsh. Chem.* **1966**, *97*, 429.

(5) Wells, R. L.; Collins, A. L. *Inorg. Chem.* **1966**, *5*, 1327.

(6) Wells, R. L; Collins, A. L. *Inorg. Nucl. Chem. Lett.* **1966**, *2*, 201.

(7) Wells, R. L.; Collins, A. L. *Inorg. Chem.* **1968**, *7*, 419.

(8) Harris, D. H.; Lappert, M. F. *J. Organomet. Chem.* **1976**, *13*, C1.

(9) Bowser, J. R.; Neilson, R. H.; Wells, R. L. *Inorg. Chem.* **1978**, *17*, 1882.

(10) Graham, D. M.; Bowser, J. R.; Moreland, C. G.; Neilson, R. H.; Wells, R. L. *Inorg. Chem.* **1978**, *17*, 2028.

(11) Paciorek, K. J. L.; Kratzer, R. H.; Kimble, P. F.; Nakahara, J. H.; Wynne, K. J.; Day, C. S. *Inorg. Chem.* **1988**, *27*, 2432.

(12) Shaw, S. Y.; DuBois, D. A.; Watson, W. H.; Neilson, R. H. *Inorg. Chem.* **1988**, *27*, 974.

(13) Jenne, H.; Niedenzu, K. *Inorg. Chem.* **1964**, *3*, 68.

(14) Nöth, H.; Sprague, M. J. *J. Organomet. Chem.* **1970**, *22*, 11.

(15) Nöth, H.; Storch, N. *Chem. Ber.* **1974**, *107*, 1028.

(16) Shriver, D. F.; Drezdzon, M. A. *Manipulations of Air Sensitive Compounds*, 2nd ed.; Wiley: New York, 1986.

(17) Ohashi, O.; Kurita, Y.; Totani, T.; Watanabe, H.; Nakagawa, T.; Kubo, M. *Bull. Chem. Soc. Jpn.* **1962**, *35*, 1317.